


RESEARCH ARTICLE

High-resolution peat volume change in a northern peatland: Spatial variability, main drivers, and impact on ecohydrology

Jelmer J. Nijp^{1,2,3,4}  | Klaas Metselaar² | Juul Limpens¹ | Harm M. Bartholomeus⁵ | Mats B. Nilsson⁶ | Frank Berendse¹ | Sjoerd E.A.T.M. van der Zee^{2,7}

¹ Plant Ecology and Nature Conservation Group, Wageningen University, Wageningen, The Netherlands

² Soil Physics and Land Management Group, Wageningen University, Wageningen, The Netherlands

³ Soil Geography and Landscape Group, Wageningen University, Wageningen, The Netherlands

⁴ Ecohydrology Department, KWR Watercycle Research, Nieuwegein, The Netherlands

⁵ Laboratory of Geo-information Science and Remote Sensing, Wageningen, The Netherlands

⁶ Department of Forest Ecology and Management, Swedish University of Agricultural Sciences, Umeå, Sweden

⁷ School of Chemistry, Monash University, Melbourne, Victoria, Australia

Correspondence

J.J. Nijp, Groningenhaven 7, Postbus 1072, 3430 BB. Nieuwegein, The Netherlands.
Email: jelmer.nijp@kwrwater.nl

Funding information

WIMEK/SENSE (The Wageningen Institute for Environment and Climate Research, and the Socio-Economic and Natural Sciences of the Environment); Dutch Foundation for the Conservation of Irish Bogs; Schure-Beijerinck-Popping fund (KNAW)

Abstract

The depth of the groundwater table below the surface and its spatiotemporal variability are major controls on all major biogeophysical processes in northern peatlands, including ecohydrology, carbon balance, and greenhouse gas exchange. In these ecosystems, water table fluctuations are buffered by compression and expansion of peat. Controls on peat volume change and its spatial variability, however, remain elusive, hampering accurate assessment of climate change impact on functioning of peatlands. We therefore (1) analysed patterning of seasonal surface elevation change at high spatial resolution (0.5 m); (2) assessed its relationship with vegetation, geohydrology, and position within the peatland; and (3) quantified the consequences for peatland surface topography and ecohydrology. Changes in surface elevation were monitored using digital close-range photogrammetry along a transect in a northern peatland from after snowmelt up to midgrowing season (May–July). Surface elevation change was substantial and varied spatially from −0.062 to +0.012 m over the measurement period. Spatial patterns of peat volume change were correlated up to 40.8 m. Spatial variation of peat volume change was mainly controlled by changes in water table, and to a lesser extent to vegetation, with peat volume change magnitude increasing from lawn < hollow < flark. Our observations suggest that patchiness and vertical variability of peatland surface topography are a function of the groundwater table. In dry conditions, the variability of surface elevation increases and more localized groundwater flows may develop. Consequently, spatially variable peat volume change may enhance peatland water retention and thereby sustain carbon uptake during drought.

KEYWORDS

compression, ecohydrology, geostatistics, groundwater, peat volume change, peatlands, photogrammetry, spatial patterns

1 | INTRODUCTION

Northern peatlands are wet ecosystems in which partially decomposed organic material (peat) has accumulated over thousands of years, making these ecosystems an important store in the global carbon cycle (Kleinen, Brovkin, & Schuldt, 2012; Turunen, Tomppo, Tolonen, & Reinikainen, 2002; Yu, 2011). In these wetland ecosystems, the depth of the water table relative to the surface is a key factor controlling numerous biogeochemical processes, including greenhouse gas emissions, plant growth and competition, redox state, and water and energy partitioning (Blodau, Basiliko, & Moore, 2004; Kettridge et al., 2015; Lafleur, Hember, Admiral, & Roulet, 2005; Limpens et al., 2008; Nijp et al., 2014; Nilsson & Öquist, 2009; Peichl et al., 2013; Waddington et al., 2015).

The distance between the groundwater table and peat surface (relative groundwater table; GWT_R) is controlled by multiple ecohydrological feedbacks, which together result in a stabilization of GWT_R and surface wetness (Belyea & Baird, 2006; Waddington et al., 2015). One of the feedbacks essential in stabilizing GWT_R in northern peatlands is peat volume change (Kennedy & Price, 2005; Nijp et al., 2017; Price, 2003). Peat in northern peatlands generally consists of partially decomposed peatmosses (*Sphagnum*; Rydin & Jeglum, 2013). The open pore structure and high compressibility of this fibrous material (Price, Cagampan, & Kellner, 2005; Waddington, Kellner, Strack, & Price, 2010) enable expansion of the saturated peat matrix in wet periods and compression during dry spells (referred to as *peat volume change*). The stabilizing effect of peat volume change on GWT_R can be considerable (~0.01 to 0.28 m reduction of temporal groundwater fluctuations; Almendinger, Almendinger, & Glaser, 1986; Baden & Eggelsmann, 1964; Fritz, Campbell, & Schipper, 2008; Roulet, 1991) and effectively reduces peatmoss moisture stress (Nijp et al., 2017). From classical soil mechanics it follows that the peat volume change potential increases with larger peat compressibility and peat thickness (Almendinger et al., 1986; Schlotzhauer & Price, 1999) and that actual peat volume change is controlled by changes in mechanical effective stress (Terzaghi, 1943).

The overall development of northern peatlands is controlled by ecohydrological interactions operating at various spatiotemporal scales (Ivanov, Thomson, & Ingram, 1981; Waddington et al., 2015). Therefore, alterations in local processes (e.g., plant community) induced by changes in external factors may affect larger scale (e.g., whole peatland) processes and vice versa (Belyea, 2009; Belyea & Baird, 2006). Such cross-scale feedbacks may result in self-organized spatial structures of vegetation, mechanical and hydrophysical properties, and of peat accumulation rates (Belyea & Baird, 2006; Belyea & Clymo, 2001; Eppinga, de Ruiter, Wassen, & Rietkerk, 2009; Rydin, 1986). As direct controls on peat volume change (compressibility, peat thickness, and changes in water table depth) are indirectly affected by feedbacks at various spatiotemporal scales, it seems likely that also peat volume change is spatially structured at multiple spatial scales. Modifications in the spatial arrangement of spatial structures within northern peatlands caused by changes in external drivers may thus alter the hydrological and biogeochemical functioning (Baird, Belyea,

& Morris, 2013), which may nonlinearly feed back to the global climate (Belyea, 2009; Belyea & Baird, 2006). Monitoring modifications of such self-organized patterns may assist detecting and preventing undesired sudden and irreversible regime shifts in ecosystem functioning (Kéfi et al., 2014; Nijp et al., 2019).

The vegetation of northern peatlands regularly forms easily recognizable units in vegetation composition and function (microforms) and is commonly classified in elevated dry hummocks, wet hollows, and lawns located in between (Andrus, Wagner, & Titus, 1983; Rydin & Jeglum, 2013). As peatland microforms may persist for centuries or even millennia (Hughes, Mauquoy, Barber, & Langdon, 2000; Karofeld, 1998; Nungesser, 2003; van der Linden, Barke, Vickery, Charman, & van Geel, 2008), the composition of plant litter added to the peat surface will determine the hydrophysical characteristics of the peat matrix later formed (Belyea & Clymo, 2001). Previous studies suggest that peat volume change and compressibility are related to microform and its associated characteristics such as bulk density, and degree of decomposition (Price et al., 2005; Waddington et al., 2010). Positive feedbacks between compressibility and plant species composition seem to occur, so that spatial variation of peat volume change could be related to present microform distribution (Waddington et al., 2010; Whittington et al., 2007).

Spatially structured peat volume change patterns may furthermore arise from processes that affect the peat thickness and fluctuations in water table. The local peat thickness is related to the alignment of the peatland in the landscape and peat development over larger spatio-temporal scales (Belyea & Baird, 2006). Besides rainfall and evapotranspiration, lateral flow constitutes a major part of the peatland water balance and therefore impacts water table fluctuations and peat volume change (Kellner & Halldin, 2002; Peichl et al., 2013). Lateral water transport is controlled by the hydraulic gradient, hydraulic conductivity, and aquifer thickness (Hillel, 2004; Ivanov et al., 1981). In turn, these properties are a function of larger-scale positional variables describing the regional flow and position of the peatland in the landscape (Grootjans, van Wirdum, Kemmers, & van Diggelen, 1996; Ivanov et al., 1981; Kemmers, 1986).

In summary, many processes operating at various spatiotemporal scales may affect the magnitude and spatial organization of peat volume change. Yet, little is known about the spatial structure of peat volume change and its spatial scale of patterning. Moreover, studies establishing links between peat volume change in northern peatlands and potential drivers are rare (Waddington et al., 2010).

This study aims to (1) explore the fine-scale (0.5 m resolution) spatial structure of peat volume change patterns; (2) determine to what extent peat volume change is affected by (a) vegetation composition, (b) position in the peatland, and (c) local geohydrological factors controlled by ecohydrological landscape position; and (3) determine the effects of spatially variable peat volume change over the growing season on peatland topography and hydrology. Due to the feedbacks between changes in plant community composition and their hydrophysical characteristics (Belyea & Baird, 2006; Waddington et al., 2010), we hypothesize that vegetation composition is a good predictor of peat volume change magnitude and its spatial variability.

Using photogrammetric processing of digital images taken along a transect in a natural peatland at multiple times throughout the growing season, we obtained highly accurate, high-resolution (<0.5 m) digital terrain models (DTMs). These DTMs allowed geostatistical quantification of the spatial structure of peat surface elevation through time, and relating it to vegetation composition, positional, and geohydrological site factors.

2 | METHODS

2.1 | Site description and climate

This research was performed in Degerö Stormyr, a natural, minerogenic, oligotrophic mixed peatland complex located in northern Sweden (64°N°19E°; Figure 1). The peat is underlain by undulating acidic gneissic bedrock and glacial till material (Malmström, 1923), and ranges in thickness from 3 to 4 m, locally reaching up to 8 m. The climate is boreal (Peel, Finlayson, & McMahon, 2007), with mean (1961–1990) annual mean temperature of +1.2°C and a mean annual rainfall sum of 523 mm, of which 34% falls as snow (Alexandersson, Karlström, & Larsson-Mccann, 1991). Rainfall, potential evapotranspiration, and mean temperature during the growing season (1991–2020) are estimated at 366 mm, 263 mm, and 11.5°C (Nijp et al., 2017).

Vegetation on the study site was dominated by hollow- and lawn species (a.o. *Sphagnum majus*, *S. balticum*, *S. lindbergii*, *Eriophorum vaginatum*, and *Trichophorum cespitosum*).

2.2 | Data collection

2.2.1 | Spatially explicit peat volume change at high resolution

Within the Degerö Stormyr peatland, we used a 571-m-long and ~6-m-wide transect from the south-western peatland margin to the north-eastern margin along an existing boardwalk (Figure 1). Peatland vegetation and surface elevation are highly sensitive to (compaction by) treading, and the boardwalk provided an essential means to prevent disturbance of the peat surface. To estimate temporal peat volume change, we created a time series of DTMs of the boardwalk transect at five points in time (see Appendix 2 in the supporting information for dates and more details), in the period right after the snow-melt until the middle of the growing season (7 May to 12 July 2013). We assume that the growing season started with a saturated peat matrix, supported by the shallow groundwater tables (<0.05 m below peat surface) in May as observed in a 12-year record of groundwater (Peichl et al., 2014) and of diluted TOC concentrations measured in peatland peak discharge at the onset of the growing season (Leach,

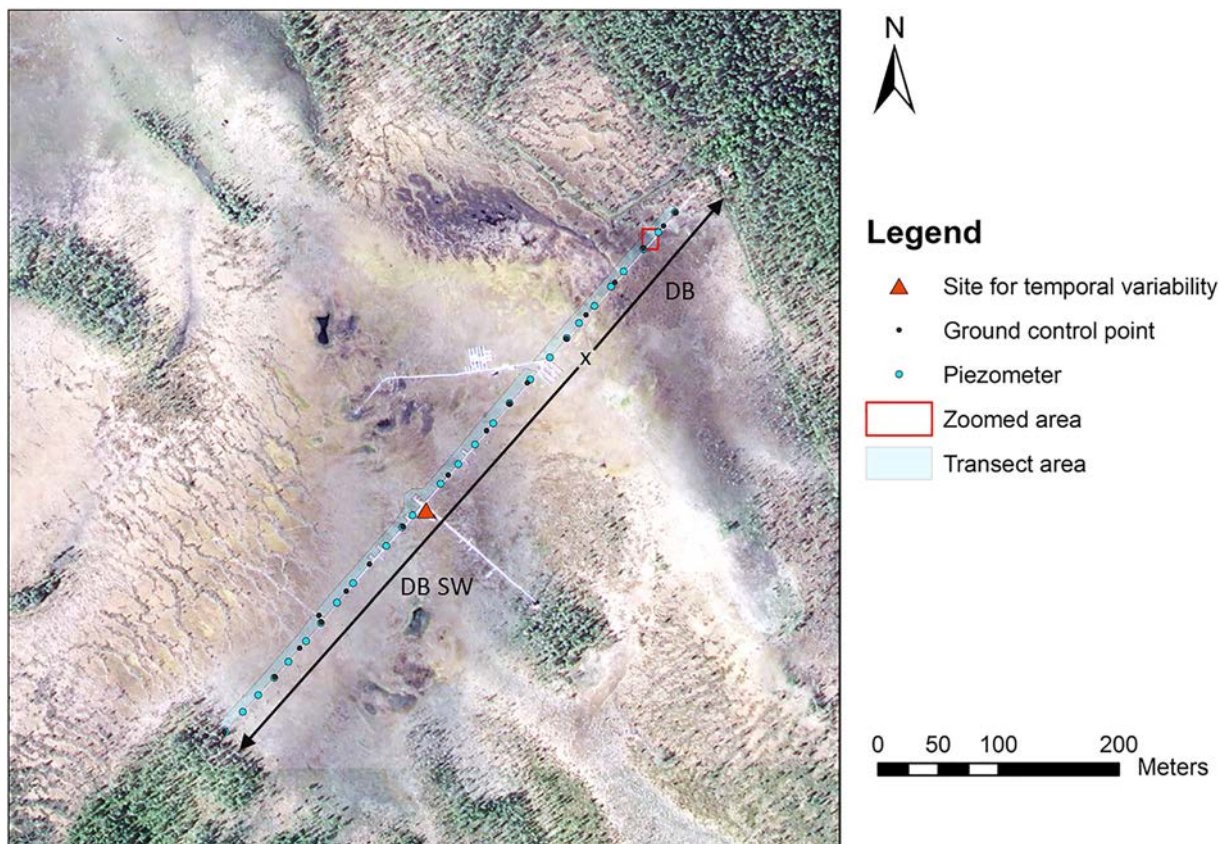


FIGURE 1 Overview of the Degerö Stormyr study site and transect of interest. The definitions of distance to nearest peat-forest border (DB) and south-western border (DB SW) from point x are illustrated with arrows. The red rectangle shows the extent of Figure 3. Aerial imagery (0.5-m resolution) was provided by © Lantmäteriet

Larsson, Wallin, Nilsson, & Laudon, 2016). As such, winter conditions reset potential water deficits accumulated in previous year's fall. DTMs were constructed from high-resolution top-view photographs taken ~6 m above the peat surface with digital close-range photogrammetry (see section 2.3). A Canon EOS 450D camera (4,272 · 2,848 pixels) with a Canon EFS 18–55 mm F/3.5–5.6 lens was attached on a 7 m-long rod.

2.2.2 | Ground survey

To georeference the constructed DTMs, we established 22 ground control points along the transect by fixing iron tubes into the underlying mineral glacial deposits, generally separated 35 m apart (Figure 1). The coordinates of the ground control points were determined using a combination of a Total Station and dGPS with a vertical accuracy of ± 7 mm. The ground control points were also used to validate peat surface elevation change in the area surrounding the tube, by manually measuring the distance between the top of the tube and the peat surface. The ground survey revealed that the peat surface along the transect sloped slightly downward in Northeasterly direction with a mean gradient of 0.0012 m/m. Refer to Appendix 4 in the supporting information for recorded coordinates and vertical positions.

During the installation of ground control points, we also verified the presence and thickness of ice. Our survey showed that only in some isolated, well-developed hummocks along the transect some small ice lenses (<0.05 m) occurred in the first half of May. Given the very low areal contribution of hummocks along the transect and the thinness of the ice lenses observed, we assumed that the effect of ice lenses on the peat surface elevation changes observed in our study is minimal and not comparable to that of the *palsa* peatlands in the more northern discontinuous permafrost zone (Petrone et al., 2008).

2.2.3 | Explanatory variables

Geohydrology

Twenty-eight piezometers were placed equidistantly along the transect (Figure 1) to estimate the depth of the water table relative to the peat surface (GWT_R ; m) and provide data from which the horizontal saturated hydraulic conductivity (K_S ; m/day) can be inferred. The piezometers consisted of cylindrical closed-bottom polyvinyl-chloride tubes (inner radius = 0.018 m) with the filter located 0.20–0.40 m below the peat surface (Appendix 1 in the supporting information). The filter of the piezometers was constructed by covering a perforated section (30% perforated area; hole diameter of 0.008 m) with a filter cloth to prevent clogging with peat debris. Groundwater table with respect to the peatmoss surface (GWT_R ; m) was measured at the five dates coinciding with image collection. A quick computation based on Darcy's law ($q = -K_S dH/dz$) suggests that the use of piezometers as groundwater wells is acceptable in used filter setting. With a minimum saturated hydraulic conductivity (K_S) of 5 m/day (see Appendix 1 in the supporting information), a maximum distance between groundwater table and bottom filter of 0.5 m (dz), and a flux of 0.01 m/day (q), the expected hydraulic head difference (dH) between

groundwater table and bottom of filter is 0.001 m. This is equal to the precision of the groundwater pressure sensors and is thus considered negligible.

We estimated the saturated horizontal hydraulic conductivity (K_S) of the 0.20- to 0.40-m-deep peat layer using in situ slug tests as described in van Dijk, Nijp, Metselaar, Lamers, and Smolders (2017). In slug tests, a volume of water (*slug*) is quickly poured into the piezometers, which generates a hydraulic head difference and induces flow from the piezometer into the peat matrix. K_S was estimated using the rate of change in the water level in the piezometer over time and piezometer flow system characteristics (Zlotnik, Goss, & Duffield, 2010). The water level in the piezometers was measured using groundwater-level loggers (Diver type DI220, Van Essen Instruments, Delft, The Netherlands). As water chemistry affects saturated hydraulic conductivity estimates (Kettridge & Binley, 2010), the slug-water (100 mL) was collected from a pool in the peatland to match local water quality. Repeated slug tests ($n = 3$) within 1 day on the same filter ($n = 7$) indicate that the mean measurement error of K_S is 5.4% of the mean observed value. This confirms the high precision that can be obtained with slug tests, in agreement with van Dijk et al. (2017).

Peat thickness (PT; m), here defined as the distance between the peatmoss surface and the peat to mineral interface at saturation (i.e., start of the growing season), was measured by pushing an extendable metal rod into the peat. The water table relative to a fixed datum, referred to as the absolute groundwater table (GWT_A), was measured in the first week of May at all piezometer locations. Changes in absolute groundwater table (ΔGWT_A) were calculated from changes in GWT_R and surface elevation inferred from DTMs.

Ecohydrological landscape position factors

The ecohydrological landscape position within a peatland may be an overall descriptor of peat thickness and water flow (Ingram, 1982; Ivanov et al., 1981) and therefore control the magnitude of peat volume change. We quantified this position with the Euclidian distance to the closest peat-forest border, to the southwest peat-forest border, and with the initial peat surface elevation above sea level, which were all derived from the ground survey data.

Vegetation

The abundance of vascular plant and bryophyte species was observed in 28 vegetation plots (0.5 · 0.5 m) centred around each of the 28 piezometers along the transect in the end of May 2013. The cover of dead plant material, bare peat, and liverwort cover (classified in living and dead) was recorded (see Appendix 4 in the supporting information for data on plant composition).

2.2.4 | Time series of peat volume change, meteorology, and groundwater table

To verify seasonal peat volume change patterns detected with photogrammetry, we monitored the temporal variation of peat surface elevation at 30-min intervals at the centre of the transect (Figure 1) with a magnetostrictive linear position sensor during the whole period (MTS

Linear Position Sensor Type CM250AVH2, MTS Sensor Technologie, Lüdenscheid, Germany). The position sensor was mounted on a frame between two iron tubes that were installed into the underlying mineral soil, providing a fixed height reference to which peat surface elevation changes could be referenced (see Nijp et al., 2017, for technical details).

Rainfall was measured with a tipping bucket rain gauge (ARG 100, Campbell, Scientific, Logan, Utah, USA, 0.0002-m resolution) near the peat volume change measurements (Figure 1). The tipping bucket records were corrected for a 10% systematic underestimation of rain amount following Eriksson (1983) in Nilsson et al. (2008). Hourly potential evapotranspiration rates were estimated from air temperature, wind speed, net radiation, and relative humidity following Food and Agriculture Organization standards (Allen et al., 2006; Allen, Raes, Pereira, & Smith, 1998). To determine the drought status from a meteorological perspective, we calculated the *cumulative potential rainfall surplus* subtracting daily potential evapotranspiration from daily rainfall (*rainfall surplus*), and adding this value to the rainfall surplus of the previous day. A half-hourly time series of GWT_R was obtained with a float- and counterweight system attached to a potentiometer (Roulet, 1991) in a lawn microform at about 200 m distance from the centre of the transect.

2.3 | Data analysis

2.3.1 | From images to peat volume change

Constructing DTMs

DTMs were created for all measurement dates using a Structure-from-Motion algorithm (Jebara, Azarbajani, & Pentland, 1999) implemented in Photoscan v1.1.2 Professional Edition (Agisoft LCC, St. Petersburg, Russia). First, a sparse point cloud was constructed by aligning the images with high accuracy, generic point selection, keypoint limit at 40,000, and tie point limit at 1,000. Misaligned images were manually realigned or removed if realignment was not successful. Next, to georeference the point cloud and remove nonlinear distortions in the constructed peat surface, camera calibration parameters and point coordinates were optimized by comparing observed coordinates of the ground control tubes obtained with the ground survey with simulated coordinates. See Appendix 2 in the supporting information for detailed information on the constructed sparse point clouds.

Points not representing the peat surface (e.g., vascular vegetation) were removed using a variant of the triangular irregular network

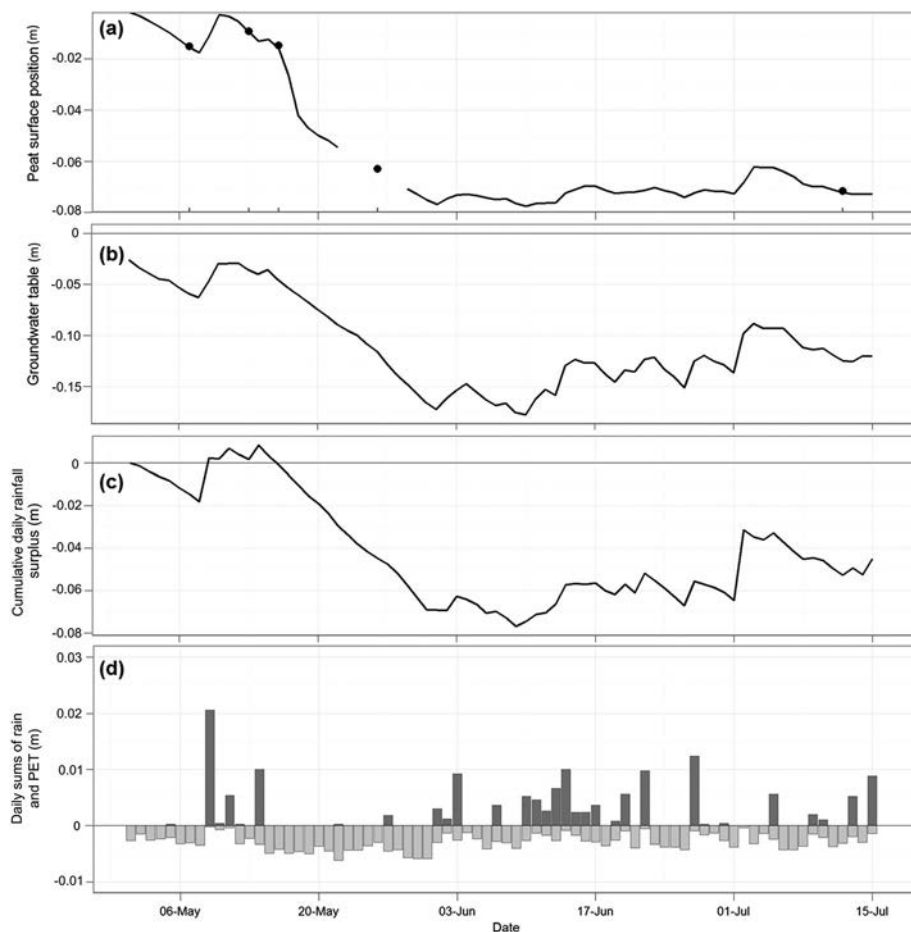


FIGURE 2 Time series of (a) peat surface position at the peatland centre, (b) water table relative to peat surface, (c) cumulative rainfall surplus, and (d) rainfall and potential evapotranspiration (PET) during the measurement period. Peat surface position is measured with a linear position sensor in the centre of the peatland; the y-axis represents the surface position relative to the first observation. Dates of transect measurements are presented with points in 1a. Rainfall, potential evapotranspiration, and cumulative rainfall surplus are daily sums. Potential evapotranspiration is calculated following Food and Agriculture Organization standards (Allen et al., 1998)

refinement algorithm (Axelsson, 2000) implemented in LAS Tools (version 150406, Rapidlasso GmbH, Gilching, Germany). To further prevent vascular plants from biasing peat surface estimates, the lowest surface point in a regular $0.5 \cdot 0.5$ -m grid was used as peat surface proxy. All data within 1 m of human influence (e.g. boardwalks) were discarded. A high-resolution gridded dataset of peat volume change was constructed by subtracting the DTM at the wettest point in time (13 May) from the driest (12 July) to obtain the maximum seasonal peat volume change.

DTM validation

The quality of the generated DTMs was assessed in three ways. A first estimate of the quality was obtained by comparing the difference between the projected and measured coordinates at the ground control points (i.e., top of tubes installed in mineral soil) after the

photogrammetric processing. The mean error in vertical position at the ground control points was 0.0065 m, averaged over the five points in time. Second, manual peat surface position measurements at the ground control points were compared with photogrammetrically produced DTM values at the closest grid cells. The peat surface position was on average underestimated by 0.0026 m (median vertical error), and the mismatch with observations ranged between -0.024 and $+0.003$ m (25th–75th percentiles; Appendix 2 in the supporting information). The root-mean-square error between manual and photogrammetric peat elevation estimates was 0.022 m. This difference, however, also includes the manual measurement error of the distance between peat surface and top of ground control tube. Third, to determine how the quality of the DTMs is affected by the proximity to ground control points, we sequentially removed ground control points

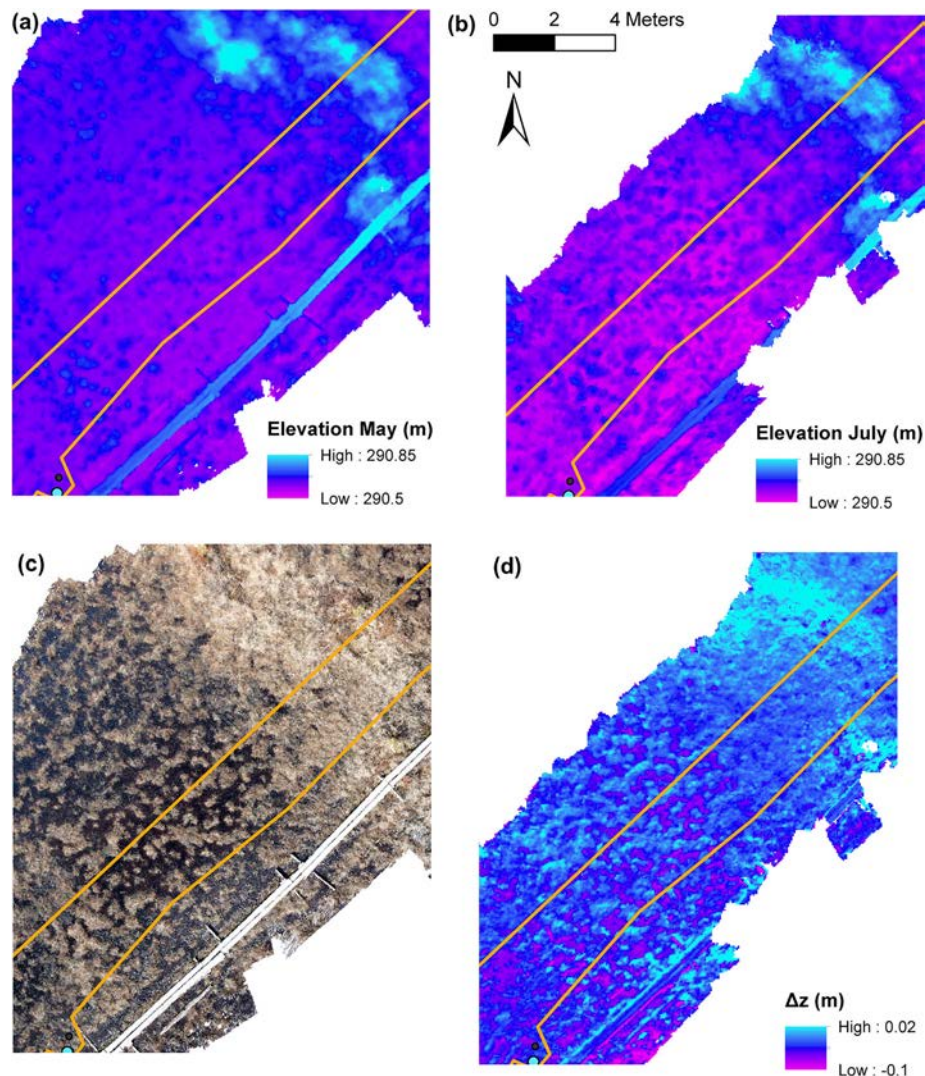


FIGURE 3 Illustrating the strength of digital photogrammetry for quantifying high-resolution surface elevation and peat volume change for section of transect. (a) High-resolution (0.05 m) spatial variability of peat surface elevation at 16 May and (b) 12 July. (c) Orthophoto (0.02-m resolution) taken at 16 May showing the fine-scale variability of vegetation, with flarks (black) in between *Eriophorum vaginatum* and *Trichophorum cespitosum* tussocks (pale brown). (d) High-resolution (0.05 m) change in peat volume (May–July); negative numbers denote compression of the peat matrix. The yellow lines delineate the area of which data were used for all spatial analyses. On all figures, a hummock string with higher elevation in the northeast and boardwalks are clearly distinguished, as well as finer scale *Eriophorum vaginatum* and *Trichophorum cespitosum* tussocks

closest to a ground control point in the centre of the transect (Appendix 2 in the supporting information). This test demonstrated that at the mean separation distance from a ground control point along the transect (35 m), the vertical error was maximally 0.007 m. The distance between ground control points was thus appropriately chosen.

2.3.2 | Spatial analysis of peat volume change patterns

Variograms were calculated to quantify spatial heterogeneity of peat volume change in terms of patchiness, variability, and random versus spatially structured components. Briefly, a variogram assesses how spatial autocorrelation changes as a function of distance (Journel & Huijbregts, 1978; Webster & Oliver, 2007). The distance up to which a variable is spatially autocorrelated is referred to as correlation range and represents the characteristic *patch size* (Webster & Oliver, 2007). Consistent with geostatistical terminology we refer to *sill* ($C+C_0$) as the asymptotic value of the variance, which provides a measure of *variability* (range of values) encountered along the transect. Due to random noise, measurement error, and variability occurring at distances smaller than the separation distance, a random component may be added to the variogram, referred to as *nugget variance* (C_0). The spatially structured component of the sill is referred to as the *partial sill* (C ; see Appendix 3 in the supporting information for details). To identify whether peat volume change was predominantly spatially structured or randomly distributed, we calculated the relative structural variance, expressed as $C/(C+C_0)$; Cirkel, Witte, van Bodegom, Nijp, & van der Zee, 2014).

As variogram calculations are sensitive to outliers (Rossi, Mulla, Journel, & Franz, 1992; Webster & Oliver, 2007), we removed surface elevation outliers (defined as values smaller than $Q_{25} - 1.5 \cdot \text{IQR}$ or larger than $Q_{75} + 1.5 \cdot \text{IQR}$, where Q_{25} and Q_{75} are the 25th and 75th quantiles and IQR the interquartile range sensu Hoaglin, Iglewicz, and Tukey (1986)). To meet the requirement of second order stationarity (i.e., mean and variance do not change in space),

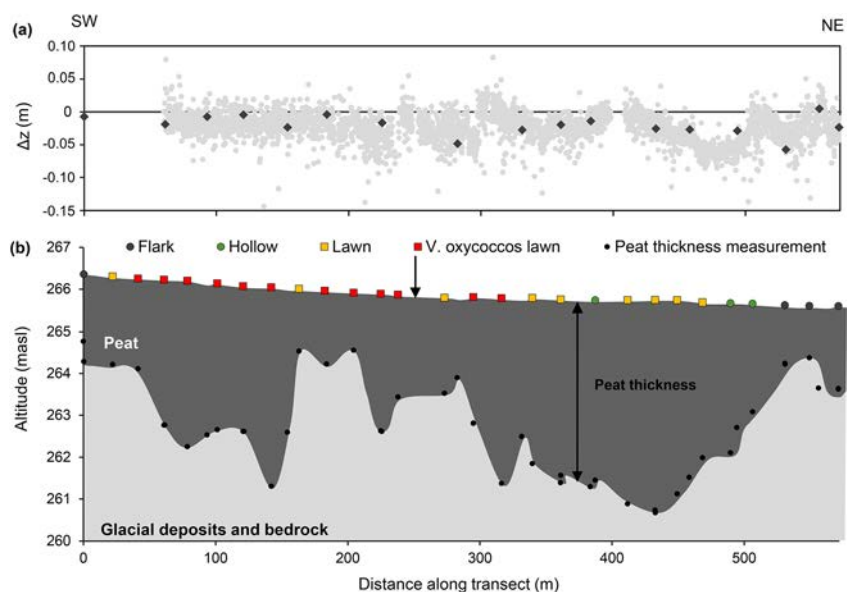
we removed the systematic trend with a second-order polynomial trend surface. Spherical, exponential, and Gaussian theoretical variogram models were fitted through the empirical variogram based on trend-removed residuals using a weighed nonlinear least squares algorithm with the *gstat* package (Pebesma, 2004) in R v3.1.0 (R Core Team, 2018). Linear combinations of up to three variograms models were also tested because empirical variograms indicated the presence of multiple spatial scales (see Appendix 3 in the supporting information for details). The Akaike Information Criterion (Akaike, 1973) was used to select the model describing the spatial structure best with least parameters. To determine how patterns in surface elevation changed with drier conditions, we also constructed variograms of peat surface elevation for all dates.

2.3.3 | Vegetation: Correspondence analysis and clustering

Correspondence analyses were used to determine whether the magnitude of peat volume change was related to vegetation composition or other environment variables. We first employed principal component analysis to explore environmental variables explaining vegetation composition using the CANOCO software (v5.0; Biometris, Plant Research International, Wageningen, The Netherlands; ter Braak and Šmilauer (2012)). Next, the effect of peat volume change on vegetation composition was quantified and tested with an unrestricted Monte Carlo Permutation Test (999 permutations).

To group the vegetation relevés to coarser-scale microforms, we used hierarchical agglomerative clustering with Euclidian distance as distance measure and Ward's minimum variance method as clustering algorithm using the *pvclust* package in R (Suzuki & Shimodaira, 2006). A multiscale nonparametric bootstrapping resampling procedure (10,000 bootstrap replications) was performed to estimate the uncertainty of the hierarchical clustering and determine the number of significantly distinct clusters (Suzuki & Shimodaira, 2006).

FIGURE 4 (a) Peat volume change along the transect during the period 16 May to 12 July from southwest (left) to northeast (right). Negative values represent compression, positive values expansion. The grey points represent peat volume change obtained by digital photogrammetry in a 2 m-wide area along the transect; the black diamonds represent ground control tube positions. (b) Peat thickness and sampling locations along the transect. The dark grey is peat; the pale grey is mineral soil. The piezometer locations are presented with dots. The lines are rough interpolations of peat depth and peat surface; the arrow indicates the position at which the peat volume change time series was obtained



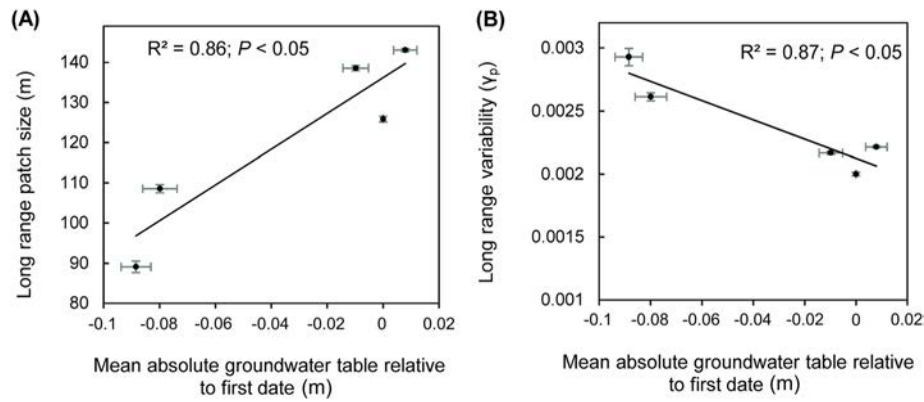


FIGURE 5 Relation between (a) absolute water table depth (GWT_A) and patch size of surface elevation and (b) peat surface position vertical variability as derived from geostatistical analyses. The x-axis represents GWT_A relative to the first observation averaged over the 28 observations, for each point in time. Mean patch size and variability of surface elevation represent the fitted practical correlation range and partial sills, obtained with a combined exponential-Gaussian variogram model fitted on the digital terrain model data. The error bars represent one standard error

3 | RESULTS

3.1 | Temporal patterns of peat volume change

Peat surface elevation decreased over the study period (Figure 2a) and generally followed the changes in the water balance as expressed by the water table relative to the peat surface (Figure 2b) and the cumulative potential rainfall surplus (Figure 2c). The total rainfall amount during the measurement period (224 mm in the period May–July) was representative for the longer term average (Nijp et al., 2015). From 15 May until 1 June a warm and dry period with mean temperature of 15.5°C (long-term average (2001–2011) average May temperature is 7.4°C) and only 0.002 m of rainfall resulted in high potential evapotranspiration rates and a rapidly increasing cumulative potential rainfall deficit (i.e., rainfall deficit that would have occurred if evapotranspiration is at its potential rate; Figures 2c and 2d). As a consequence of this dry period, the peat surface at the centre of the peatland dropped by nearly 0.08 m.

3.2 | Spatial structure of peat volume change

Changes in peat surface elevation along the transect were highly variable in space (Figures 3d and 4a and Appendix A2.3 in the supporting information). The median change in peat volume between the wettest (13 May 2013) and driest (12 July 2013) point in time was -0.031 m, with values ranging from $+0.012$ to -0.062 m (5th and 95th quantiles). Peat volume change was clearly spatially structured (Figure 3d and Appendix A2.3 in the supporting information). Indeed, the high relative structural variance (see section 2.3.2) of 74% indicates that most of the high-resolution (0.5 m) spatial variation in peat volume change can be attributed to spatially structured properties rather than to random properties. Two spatial scales of patterning were present, as suggested by the combined exponential-Gaussian variogram model describing the spatial structure of peat volume change best with least

parameters (Appendix 3 in the supporting information). The two spatial scales of patterning were 3.4 ± 0.8 m (short-range; mean correlation range \pm standard error) and 40.8 ± 0.6 m (long-range). Even though the combined variogram model had the best fit, the short-range pattern was not significant ($p = .16$) and the long-range (Gaussian) model component explained most (78%) of the spatially structured variation in peat volume change. Spatial patterns, that is, characteristic patch size of peat volume change, were thus best described at a spatial scale of 40.8 m.

3.3 | Spatiotemporal changes in surface topography

Spatial patterns in peat surface elevation at the five points in time emerged at a short-range (3.68 ± 0.22 m [\pm SD]) and long-range (121 ± 22 m). Surface topography was clearly spatially structured (Figures 3a and 3b and Appendix A2.3 in the supporting information), as the short-range and long-range patterns explained 20% and 73% of the spatial variation in peat surface elevation, leaving only 7% random spatial variation. With deeper space-averaged absolute water tables, the patch size (i.e. area within which values are correlated) and vertical variability of peat surface elevation decreased (-44%) and increased (27%) significantly for the long-range spatial pattern of surface elevation (Figure 5). This indicates that surface elevation differences became more pronounced with drier conditions (i.e. later in the growing season) and that peat volume change becomes more local with deeper absolute water table. The variogram parameters of the short-range surface elevation pattern did not differ between points in time and were therefore excluded from the analyses.

3.4 | Variables correlated to peat volume change

3.4.1 | Positional and geohydrological factors

Spatial patterns of peat volume change were most closely related to changes in absolute water table (aquifer thickness), with larger changes

TABLE 1 Spearman Rank-Order Correlation Coefficients Between Peat Volume Change (Δz), Positional and Geohydrological Variables, and Its Relation to (Changes in) Groundwater Table Relative to Peat Surface (GWT_R)

Variable	Positional and geohydrological factors						Relative groundwater table		
	Elevation	DB	DB SW	PT	K_S	ΔGWT_A	GWT_R May	GWT_R July	ΔGWT_R
Δz	-0.32	0.13	0.37	0.03	-0.25	-0.73	0.01	0.41	0.46
Elevation		-0.29	-0.99	-0.29	-0.13	-0.06	0.03	-0.44	-0.46
DB			0.15	0.35	0.24	-0.03	-0.20	-0.08	-0.07
DB SW				0.10	-0.08	0.08	0.00	0.54	0.57
PT					0.58	-0.09	-0.37	-0.32	-0.16
K_S						-0.08	-0.07	-0.21	-0.24
ΔGWT_A							-0.12	0.01	0.12
GWT_R May								0.38	-0.01
GWT_R July									0.87

Note. Significant correlations ($p < .05$) are indicated in bold; Δz : Peat volume change (more shrinkage = larger positive value); m; Elevation: Peat surface elevation with respect to sea level (m asl); DB: Euclidian distance to South-western peat-forest border (m); DB SW: Euclidian distance to closest peat-forest border (m); PT: Initial peat thickness; distance between peat surface and mineral soil (m); K_S : Saturated hydraulic conductivity (m/day); ΔGWT_A : Change in absolute water level between 13 May and 12 July; more negative values indicate larger decline in absolute water level. Equals change in aquifer thickness; GWT_R May: Groundwater table relative to peat surface on 13 May (m; negative if below peat surface); GWT_R July: Groundwater table relative to peat surface on 12 July (m; negative if below peat surface); ΔGWT_R : GWT_R May – GWT_R July (m; more negative values indicate larger water level decline).

in absolute water table resulting in larger peat volume change (Table 1 and Figure 6). Peat thickness, hydraulic conductivity (see Appendix 1 in the supporting information), and distance to the (closest) peat-forest margin were not related to changes in peat surface elevation. The average hydraulic conductivity along the transect was 22.9 m/day at 21 May and did not significantly decrease when the growing season progressed (Appendix 1 in the supporting information).

Peat volume change stabilized the distance between the peat surface and GWT_R , buffering on average 26% and maximally 84% of the GWT_A decline of 0.09 m between 13 May and 12 July. Spatial variation in decline of GWT_A through time was unrelated to the position in peatland, as expressed by the global surface elevation and distance from the peat-forest margin (Table 1).

Locations in the peatland with the largest compression corresponded to sites with shallow relative water tables during the peak of the growing season (July GWT_R ; Table 1). The decline of GWT_R over the growing season was largest for sites with deep July GWT_R (Table 1), illustrating that dry sites became drier. This is consistent with the analyses on the spatial structure of topography, which indicated that patchiness and variability of peat surface elevation increased with deeper absolute water tables (Figure 5).

3.4.2 | Vegetation in relation to peat volume change

Microform level

Four microforms were distinguished based on the hierarchical cluster analysis. The first microform consisted of flarks (sensu Sjörs, 1948), characterized by liverworts (mainly *Gymnocolia inflata* and *Cladopodiella fluitans*), *Trichophorum cespitosum* and *Sphagnum papillosum*, and bare peat (Figure 2). The second class represents hollow vegetation, characterized by the species *Sphagnum majus* and *Scheuchzeria palustris*. The two remaining classes were represented

by lawn vegetation with high abundance of *Sphagnum balticum*, *Eriophorum vaginatum*, and *Andromeda polifolia*, with a high cover of *Vaccinium oxycoccos* differentiating the two lawn communities.

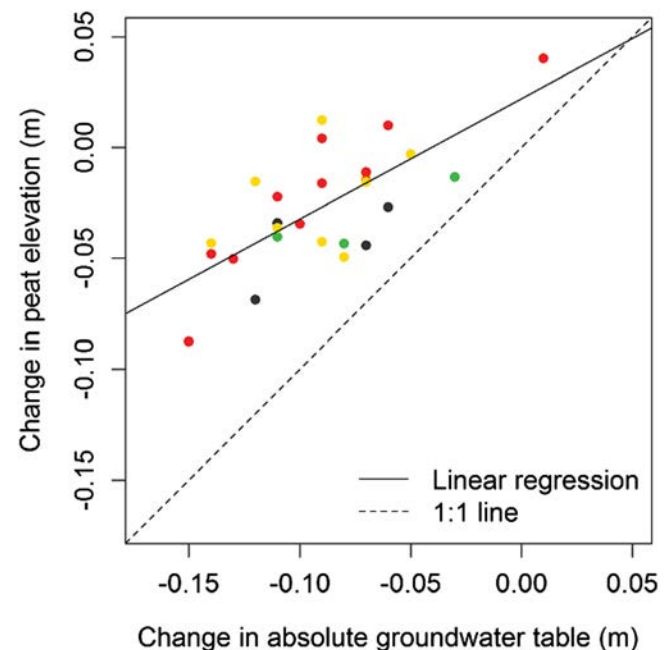


FIGURE 6 Relation between changes in absolute water table (i.e., changes in aquifer thickness) and peat surface elevation over the period 13 May to 12 July. Negative peat volume change values indicate compression; positive values indicate expansion of the saturated peat matrix. The parameters in the linear regression ($z = -0.55 \cdot \text{GWT}_A - 0.022$) were significant ($p < .05$) and the goodness of fit is 0.51 (R^2_{adj}). The colours represent vegetation classes (red = high lawn, orange = low lawn, green = hollow, and grey = flark)

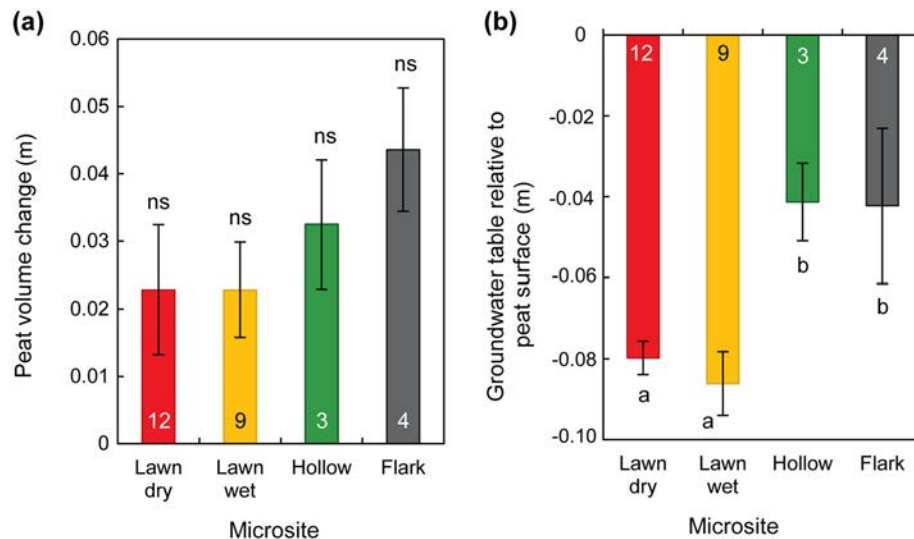


FIGURE 7 (a) Mean peat volume change per microsite between 13 May to 12 July and (b) mean water table relative to peat surface per microsite. Significant subgroups are presented with letters; ns = not significant ($p > .05$). p values are corrected following Benjamini and Hochberg (1995). The error bars represent standard errors, and the numbers in the bars are the number of replicates per microsite

The magnitude of peat volume change differed among the four identified microforms, with flarks having 90% larger shrinkage than the lawn microforms (Figure 7a). Although substantial, these differences were not statistically significant (analysis of variance [ANOVA]; $F = 0.71$, $P = 0.55$). The four microforms as established by the cluster analysis were mainly separated along the water table gradient (Fig. 8), with hollows and flarks prevailing at sites with shallower GWT_R (ANOVA; $F = 6.1$, $p < .001$; Fig. 7b).

Plant community composition level

Peat volume change explained only 7.3% (R^2) of the total variation in plant species composition, and its effect was not significant (Monte Carlo permutation test; $F = 2.0$, $p = .13$). The groundwater table relative to the peat surface (GWT_R) in July explained 30.5% ($F = 11.4$; $p < .01$) of the total variation in plant species composition and was the main explanatory factor for spatial variation in vegetation composition along the transect (Figure 8). However, due to the collinearity of GWT_R in July with ΔGWT_R , peat volume change, distance from the peat-forest border, and surface elevation, its effect on plant species composition cannot be separated from these factors (Table 1).

Despite the lack of a direct relation between peat volume change and overall vegetation composition, the magnitude of peat volume change was related to abundance of individual species. Higher abundance of *Drosera rotundifolia* was indicative for sites with large surface elevation fluctuations (Spearman correlation coefficient $\rho = .50$; $p < .05$). Plant species indicative for a low magnitude of peat volume change were *Vaccinium uliginosum* ($\rho = -.44$; $p < .05$) and *Eriophorum vaginatum* ($\rho = -.39$; $p < .05$). *Trichophorum cespitosum* ($\rho = .33$; $p < .1$) and *Sphagnum balticum* ($\rho = -.33$; $p < .1$) were also suggestive of large and small peat volume change magnitude, respectively, along the transect. See Appendix 4 in the supporting information for compositional data for vegetation plots.

4 | DISCUSSION

4.1 | Spatial structure of peat volume change patterns

This is, to our knowledge, the first analysis of the fine-scale spatial structure of peat volume change patterns within a peatland. In Degerö Stormyr, the northern peatland complex studied, spatial peat volume change is spatially correlated up to a distance of 40.8 ± 0.6 m (\pm SE), which represents the scale of peat volume change patchiness. The magnitude of peat volume change observed in the studied peatland (up to 0.062 m, from start-middle growing season) is in the range found for *Sphagnum*-dominated ombrotrophic peatland systems in the boreal and temperate zone, generally ranging between 0.02 and 0.11 m (Almendinger et al., 1986; Nijp et al., 2017; Price, 2003; Schlotzhauer & Price, 1999; Uhden, 1967; Whittington et al., 2007).

The result that spatial peat volume change patterns emerge at a spatial scale of about 40 m indicates that peatland simulation models based on horizontally uniform peat volume change can represent a limited area only. Instead, peatland hydrological models need to accommodate for spatial differences of peat volume change. Berne, Delrieu, Creutin, and Obled (2004) and Schilling (1991) suggest the measurement resolution for autocorrelated data to be 3–4 times smaller than the scale of pattern formation to adequately capture the spatial process. Accordingly, a grid resolution of about 12–15 m would be required in spatially explicit peatland hydrology models to capture peat volume change (Kennedy & Price, 2004; Nijp et al., 2017) for peatland systems comparable to Degerö Stormyr, that is, mixed mires or aapa mires. Given the strong correlation between peat volume change and groundwater dynamics (Table 1), this recommendation is likely also applicable for groundwater flow simulations in peatlands in general.

positional factors. A research setup with the transect positioned in the dominant flow direction or unmanned aerial vehicle-based survey covering both planar directions is therefore recommended for future studies.

4.3 | Vegetation composition as predictor of peat volume change?

Previous studies indicate that the compressibility and magnitude of peat volume change may differ among microforms (Roulet, 1991; Waddington et al., 2010; Whittington & Price, 2006). Along the studied transect, flarks and hollows seemed to represent peat volume change 'hotspots' (Figure 7a) at the microform level, although differences in peat volume change were not statistically significant among microforms. In contrast to our hypothesis, plant species abundance was not related ($R^2 = .073$; $p < .05$) to peat volume change in the studied peatland. This seems to suggest that the positive feedback between peat volume change and microform distribution in the studied peatland is weak. However, the lack of relationship may be attributed to (a) the low number of replicates per microform ($n = 3$) for hollows; (b) the limited variability of vegetation along the transect, particularly the absence of species of well-developed hummocks (Figure 1); and (c) faster turnover rate of species as compared with peat physical traits, resulting in the poor relation between current microform distribution and current physical properties.

An indirect positive feedback between vegetation, peat volume change, and water table depth may, however, still arise as follows. Despite the large lowering in absolute groundwater level at dry microforms, the observed surface elevation change was small as compared with wet microforms (Table 1 and Figure 7b). This suggests that dry microforms have a lower compressibility, as also reported by Waddington et al. (2010). The low compressibility at dry microforms reduces the peat volume change magnitude, leading to deep relative water table upon drying, as supported by observations in the midgrowing season (GWT_R July; Table 1). Deeper water tables promote the establishment of species adapted to deep water tables (Luken, 1985; Rydin, 1986), which, due to their low compressibility, may further decrease peat volume change magnitude. These positive feedbacks hint towards a coevolution between vegetation and peat compressibility.

At a species level, *Drosera rotundifolia* and *Trichophorum cespitosum* may be indicative for peat volume change "hotspots." Yet, as *D. rotundifolia* and *T. cespitosum* reach low cover only, their contribution to peat hydrophysical characteristics later formed by their litter can only be marginal. The correlation is therefore likely indicative of flark presence rather than suggestive of a direct relation between compressibility and vegetation composition. Abundance of *Vaccinium uliginosum* and *Eriophorum vaginatum* is moderately negatively correlated with peat volume change. In a nearby peatland, vegetation composition remained practically unchanged during the last 70 years, so that the peat material of the top 0.30 m is composed of the same plant species (van der Linden et al., 2008). Given that both peatlands

remained undisturbed during this period, it seems likely also in Degerö Stormyr that the vegetation remained unchanged. With this assumption, the correlation suggests that plant litter or roots of these plant species increased the rigidity of the peat matrix and thereby reduce its compressibility. The low sample size makes these results speculative, and using these species as indicators for peat volume change "hot spots" requires confirmation with other peatland sites before application.

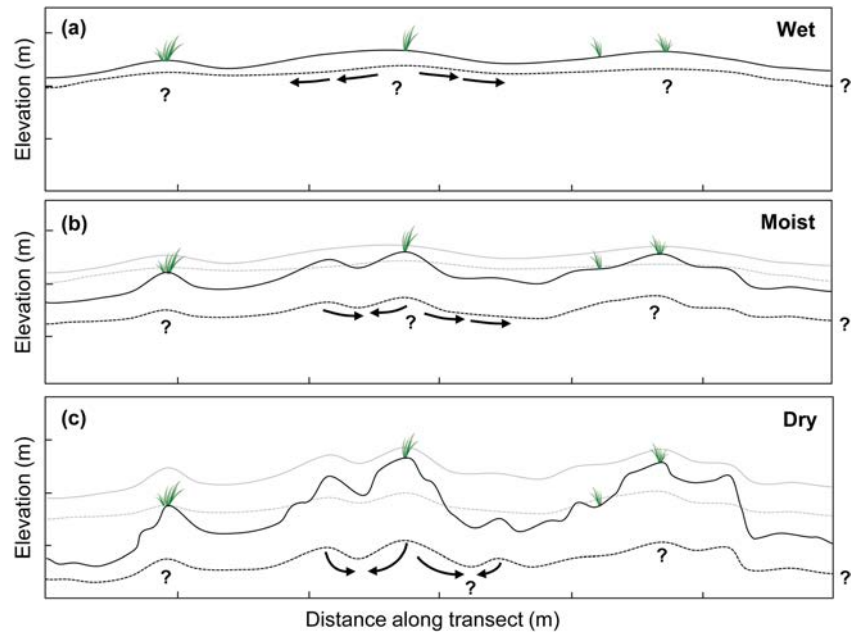
4.4 | Effects of peat volume change on surface topography

The surface topography of the studied peatland was spatially structured, with 73% of the surface patterns originating at a spatial scale of 90–140 m and 20% at about 4 m. In a UK raised bog, microtopographical hummock-hollow patterns emerged at a spatial scale of 1–4 m (Anderson, Bennie, & Wetherelt, 2010), similar to the short-range pattern scale found in our study. Given that the short-range patch size remained constant over the growing season, it seems likely that the short-range pattern is related to microform identity.

Our study suggests that reduced overall peatland wetness over time reduced the patch size and increase vertical variability of peat surface elevation within the studied peatland (Figure 5). Spatial variation in peat volume change within the peatland was mainly related to spatially variable changes in absolute water table (Table 1), suggesting that although progressively more sites became compressed with deeper water tables, the surface topography of other sites remained more stable due to differential compression (Waddington et al., 2010; Whittington & Price, 2006; Figure 9). As a result, topographical differences became more pronounced and more patchy, and also the variance of water table depth relative to the peat surface (GWT_R) will increase (Figure 9). Such increased habitat variability may increase species richness and thereby enhance peatland carbon sink stability and resilience to environmental extremes, such as droughts (Korrensalo et al., 2017; Loreau et al., 2001; Peterson, Allen, & Holling, 1998; Scherrer & Körner, 2011).

Additionally, the increased topographical variability with increased peatland drought status may affect lateral groundwater flow direction and rate. In unconfined aquifers, the water table is frequently assumed to follow topography (Desbarats, Logan, Hinton, & Sharpe, 2002; Hoeksema et al., 1989; Sonnentag, Chen, Roulet, Ju, & Govind, 2008), which is confirmed for an ombrotrophic temperate bog (Malhotra, Roulet, Wilson, Giroux-Bougard, & Harris, 2016). This would imply that with increased vertical variability and horizontal patchiness of surface elevation, the patchiness of GWT_R may also increase, resulting in temporarily steeper and more local hydraulic gradients. This may potentially lead to localized groundwater flows from elevated sites to low sites during drought, enhancing the ecohydrological differentiation between wet and dry sites. Oosterwoud, Ploeg, Schaaf, and van der Zee (2017) and Quinton and Roulet (1998) demonstrated the importance of microform variation in regulating the connectivity of overland flow, which decreased with

FIGURE 9 (a–c) Hypothetical conceptual model of peat volume change impact on topography and hydrology during progressive drying. The horizontal axis represents a horizontal transect through a peatland; the vertical axis represents the (exaggerated) position of peat surface elevation (solid black lines) and water table (dashed black lines). Groundwater flow paths are indicated with arrows and peat surface and groundwater positions in previous conditions in grey. Considering compression during the growing season, the peat elevation decreases at all positions through space upon drying (b and c). Due to spatial variability in lateral groundwater flow and peat substrate compressibility along the transect, some places start to compress earlier and more than others, enhancing the vertical and horizontal topographical heterogeneity. As a result of the increased vertical range of topography, hydraulic gradients may hypothetically become steeper and groundwater flow more local, as is illustrated with the flow lines



deeper water tables. We hypothesize that also more localized groundwater flows induced by spatially variable peat volume change may reduce hydrological connectivity. Such reduced connectivity would lead to more tortuous flowpaths and increase peatland water retention. As such, spatially different peat volume change yields another feedback mechanism to sustain peatland carbon uptake under drought, complementary to reduced hydraulic conductivity at greater depth as a result of compression (Whittington & Price, 2006). Moreover, the retention of local water may impede the inflow of minerogenic water and sustain or enhance ombrotrophy in peatlands with minerogenic water input.

The increased lateral discharge from elevated sites to lower depressions may thus amplify a positive feedback between microform compressibility and species composition and promote the spatial self-organization of vegetation patterns. As locations with deeper July GWT_R have a larger decline in GWT_R during the growing season (Table 1), our data seem to support this hypothesis. However, this suggested impact of peat volume change on redistribution of groundwater flow needs to be tested in future studies using a denser piezometer network. Moreover, although the assumption that the water table follows peatland topography (Haitjema & Mitchel Bruker, 2005) at a spatial scale from 90 to 140 m seems reasonable (Fraser, Roulet, & Lafleur, 2001; Malhotra et al., 2016), it should be verified under different geohydroclimatic conditions.

5 | CONCLUSION AND IMPLICATIONS

Using a novel approach to construct spatially continuous high-resolution (0.5 m or higher) DTMs, our results clearly show that peat volume change is spatially structured for the studied fen, with a characteristic length scale of 40.8 ± 0.6 m (\pm SE). In contrast to previous

research (Almendinger et al., 1986; Waddington et al., 2010; Whittington & Price, 2006), we found only a weak direct relation between peat volume change and microform or ecohydrological position in the peatland. Instead, spatially variable peat volume change was mainly related to changes in absolute water table, likely originating from lateral groundwater redistribution. Surface topography had a patch size of about 140 m at the start of the growing season but decreased to 90 m in the middle of the growing season, when deeper water tables occurred. In addition, the vertical variability increased with deeper water tables. We hypothesize that the increased topographical heterogeneity with deeper water tables may result in a more local redistribution of groundwater from elevated sites to depressions. This may further enhance microform patterning and the contrast between wet and dry sites during droughts and boosts peatland water retention. This hypothesis needs to be tested in other peatlands and various hydro-climatological settings. Here, the Structure-from-Motion technique was successfully applied to capture temporal changes in peat surface topography with a median vertical difference of 0.0026 m. The spatial scale of peat volume change identified in this study has direct implications for the spatial representativeness of spatially implicit simulation models that include peat volume change (Kennedy & Price, 2004; Nijp et al., 2017).

Like other self-regulating ecosystems, northern peatlands may respond nonlinearly to external perturbations and rapidly shift to a virtually irreversible, undesired state (Hilbert, Roulet, & Moore, 2000; Rietkerk, Dekker, de Ruiter, & van de Koppel, 2004; Scheffer, Carpenter, Foley, Folke, & Walker, 2001). This would imply that peatlands may potentially shift from a net carbon sink to source, feeding back to the global climate by altering radiative forcing (Bridgman, Pastor, Dewey, Weltzin, & Updegraff, 2008; Frolking & Roulet, 2007; Frolking, Roulet, & Fuglestad, 2006). Based on observations, our

study illustrates that spatial feedbacks between peat volume change, vegetation, and hydrology may enhance the resilience of peatlands to climate change.

ACKNOWLEDGEMENTS

We are thankful to Gijs van Dijk, Lena Jonsson, and Pernilla Löfvenius for assistance in the field and taking top-view images; Mattias Eklund for surveying ground control points; and Mikael Ottosson-Löfvenius for kindly providing hydro- and meteorological data. Juha Suomalainen is acknowledged for his involvement in photogrammetric analyses. This study was co-funded by the Schure-Beijerinck-Popping fund (KNAW), the Dutch Foundation for the Conservation of Irish Bogs, and WIMEK/SENSE (The Wageningen Institute for Environment and Climate Research, and the Socio-Economic and Natural Sciences of the Environment). We are thankful to the detailed and constructive feedback of two anonymous reviewers that considerably improved the quality of the manuscript. The data that support the findings of this study are partly available in the supporting information, or from the corresponding author upon request.

FUNDING

Funding includes Schure-Beijerinck-Popping fund (KNAW), The Dutch Foundation for the Conservation of Irish Bogs, and WIMEK/SENSE (The Wageningen Institute for Environment and Climate Research, and the Socio-Economic and Natural Sciences of the Environment).

ORCID

Jelmer J. Nijp  <https://orcid.org/0000-0002-6536-9437>

REFERENCES

- Akaike, H. (1973). Information theory as an extension of the maximum likelihood principle. In B. N. Petrov, & F. Csaki (Eds.), *Second International Symposium on Information Theory* (pp. 267–281). Budapest, Hungary: Akademiai Kiado.
- Alexandersson, H., Karlström, C., & Larsson-Mccann, S. (1991). *Temperature and precipitation in Sweden 1961–1990. Reference normals (In Swedish)* (Vol. 81/1991). Norrköping, Sweden: Swedish Meteorological and Hydrological Institute (SMHI).
- Allen, R. G., Pruitt, W. O., Wright, J. L., Howell, T. A., Ventura, F., Snyder, R., ... Elliott, R. (2006). A recommendation on standardized surface resistance for hourly calculation of reference ETo by the FAO56 Penman-Monteith method. *Agricultural Water Management*, 81(1–2), 1–22. <https://doi.org/10.1016/j.agwat.2005.03.007>
- Allen, R. G., Raes, D., Pereira, L. S., & Smith, M. (1998). *Crop evapotranspiration—Guidelines for computing crop water requirements—FAO irrigation and drainage paper 56*. Rome, Italy: FAO - Food and Agriculture Organization of the United Nations.
- Almendinger, J. C., Almendinger, J. E., & Glaser, P. H. (1986). Topographic fluctuations across a spring fen and raised bog in the Lost River Peatland, Northern Minnesota. *Journal of Ecology*, 74(2), 393–401. <https://doi.org/10.2307/2260263>
- Anderson, K., Bennie, J., & Wetherelt, A. (2010). Laser scanning of fine scale pattern along a hydrological gradient in a peatland ecosystem. *Landscape Ecology*, 25, 477–492. <https://doi.org/10.1007/s10980-009-9408-y>
- Andrus, R. E., Wagner, D. J., & Titus, J. E. (1983). Vertical zonation of *Sphagnum* mosses along hummock-hollow gradients. *Canadian Journal of Botany*, 61(12), 3128–3139. <https://doi.org/10.1139/b83-352>
- Axelsson, P. (2000). DEM generation from laser scanner data using adaptive tin models. *International Archives of Photogrammetry and Remote Sensing*, XXXIII(Part B3), 85–92.
- Baden, W., & Eggelsmann, R. (1964). Der wasserkreislauf eines Nordwestdeutschen hochmoores - Eine hydrologische studie über den Einfluß von Entwässerung und Kultivierung auf den Wasserhaushalt des Königsmoores. In Tostedt/Han [GERMAN] *The water cycle of a Northwest German bog—A hydrological study on the influence of drainage and cultivation on the water balance of the Königsmoor*. Hamburg, Germany: Verlag Wasser und Boden.
- Baird, A. J., Belyea, L. R., & Morris, P. J. (2013). Upscaling of peatland-atmosphere fluxes of methane: Small-scale heterogeneity in process rates and the pitfalls of “bucket-and-slab” models. In *Carbon cycling in northern peatlands* (pp. 37–53). American Geophysical Union. <https://doi.org/10.1029/2008GM000826>
- Baird, A. J., Eades, P. A., & Surridge, B. W. J. (2008). The hydraulic structure of a raised bog and its implications for ecohydrological modelling of bog development. *Ecohydrology*, 1(4), 289–298. <https://doi.org/10.1002/eco.33>
- Belyea, L. R. (2009). Nonlinear dynamics of peatlands and potential feedbacks on the climate system. In A. Baird, L. Belyea, X. Comas, A. Reeve, & L. Slater (Eds.), *Northern Peatlands and Carbon Cycling* (pp. 5–18). Washington DC, United States: Geophysical Monograph Series, American Geophysical Union.
- Belyea, L. R., & Baird, A. J. (2006). Beyond “The limits to peat bog growth”: Cross-scale feedback in peatland development. *Ecological Monographs*, 76(3), 299–322. [https://doi.org/10.1890/0012-9615\(2006\)076\[0299:BTLPB\]2.0.CO;2](https://doi.org/10.1890/0012-9615(2006)076[0299:BTLPB]2.0.CO;2)
- Belyea, L. R., & Clymo, R. S. (2001). Feedback control of the rate of peat formation. *Proceedings of the Royal Society of London Series B-Biological Sciences*, 268(1473), 1315–1321. <https://doi.org/10.1098/rspb.2001.1665>
- Benjamini, Y., & Hochberg, Y. (1995). Controlling the False Discovery Rate: A Practical and Powerful Approach to Multiple Testing. *Journal of the Royal Statistical Society: Series B (Methodological)*, 57(1), 289–300. <https://doi.org/10.2307/2346101>
- Berne, A., Delrieu, G., Creutin, J.-D., & Obled, C. (2004). Temporal and spatial resolution of rainfall measurements required for urban hydrology. *Journal of Hydrology*, 299(3–4), 166–179. <https://doi.org/10.1016/j.jhydrol.2004.08.002>
- Blodau, C., Basiliko, N., & Moore, T. R. (2004). Carbon turnover in peatland mesocosms exposed to different water table levels. *Biogeochemistry*, 67(3), 331–351. <https://doi.org/10.1023/B:BIOG.0000015788.30164.e2>
- Boelter, D. H. (1969). Physical properties of peat as related to degree of decomposition. *Soil Science Society of America*, 33, 606–609. <https://doi.org/10.2136/sssaj1969.03615995003300040033x>
- ter Braak, C. J. F., & Šmilauer, P. (2012). *Canoco reference manual and user's guide: Software for ordination (version 5.0)*. Ithaca, NY, USA: Microcomputer Power.
- Bridgman, S. D., Pastor, J., Dewey, B., Weltzin, J. F., & Updegraff, K. (2008). Rapid carbon response of peatlands to climate change. *Ecology*, 89(11), 3041–3048. <https://doi.org/10.1890/08-0279.1>
- Ciach, G. J., & Krajewski, W. F. (2006). Analysis and modeling of spatial correlation structure in small-scale rainfall in Central Oklahoma. *Advances in Water Resources*, 29(10), 1450–1463. <https://doi.org/10.1016/j.advwatres.2005.11.003>

- Cirkel, D. G., Witte, J.-P. M., van Bodegom, P. M., Nijp, J. J., & van der Zee, S. E. A. T. M. (2014). The influence of spatiotemporal variability and adaptations to hypoxia on empirical relationships between soil acidity and vegetation. *Ecohydrology*, 7, 21–32. <https://doi.org/10.1002/eco.1312>
- Desbarats, A. J., Logan, C. E., Hinton, M. J., & Sharpe, D. R. (2002). On the kriging of water table elevations using collateral information from a digital elevation model. *Journal of Hydrology*, 255(1–4), 25–38. [https://doi.org/10.1016/S0022-1694\(01\)00504-2](https://doi.org/10.1016/S0022-1694(01)00504-2)
- van Dijk, G., Nijp, J. J., Metselaar, K., Lamers, L. P. M., & Smolders, A. J. P. (2017). Salinity-induced increase of the hydraulic conductivity in the hyporheic zone of coastal wetlands. *Hydrological Processes*, 31(4), 880–890. <https://doi.org/10.1002/hyp.11068>
- Eppinga, M. B., de Ruiter, P. C., Wassen, M. J., & Rietkerk, M. (2009). Nutrients and hydrology indicate the driving mechanisms of peatland surface patterning. *American Naturalist*, 173(6), 803–818. <https://doi.org/10.1086/598487>
- Eriksson, B. (1983). *Data concerning the precipitation climate of Sweden, mean values for the period 1951–80*. Norrköping, Sweden: Swedish Meteorological and Hydrological Institute (SMHI).
- Fraser, C. J. D., Roulet, N. T., & Lafleur, M. (2001). Groundwater flow patterns in a large peatland. *Journal of Hydrology*, 246(1–4), 142–154. [https://doi.org/10.1016/S0022-1694\(01\)00362-6](https://doi.org/10.1016/S0022-1694(01)00362-6)
- Fritz, C., Campbell, D. I., & Schipper, L. A. (2008). Oscillating peat surface levels in a restiad peatland, New Zealand—Magnitude and spatiotemporal variability. *Hydrological Processes*, 22(17), 3264–3274. <https://doi.org/10.1002/hyp.6912>
- Frolking, S., Roulet, N., & Fuglestedt, J. (2006). How northern peatlands influence the Earth's radiative budget: Sustained methane emission versus sustained carbon sequestration. *Journal of Geophysical Research: Biogeosciences*, 111(G1), G01008. <https://doi.org/10.1029/2005jg000091>
- Frolking, S., & Roulet, N. T. (2007). Holocene radiative forcing impact of northern peatland carbon accumulation and methane emissions. *Global Change Biology*, 13(5), 1079–1088. <https://doi.org/10.1111/j.1365-2486.2007.01339.x>
- Grootjans, A. P., van Wirdum, G., Kemmers, R., & van Diggelen, R. (1996). Ecohydrology in The Netherlands: Principles of an application-driven interdisciplinary. *Acta Botanica Neerlandica*, 45(4), 491–516. <https://doi.org/10.1111/j.1438-8677.1996.tb00807.x>
- Haitjema, H. M., & Mitchell-Bruker, S. (2005). Are water tables a subdued replica of the topography? *Ground Water*, 43(6), 781–786. <https://doi.org/10.1111/j.1745-6584.2005.00090.x>
- Heijmans, M. M. P. D., Arp, W. J., & Berendse, F. (2001). Effects of elevated CO₂ and vascular plants on evapotranspiration in bog vegetation. *Global Change Biology*, 7(7), 817–827. <https://doi.org/10.1046/j.1354-1013.2001.00440.x>
- Hilbert, D. W., Roulet, N., & Moore, T. (2000). Modelling and analysis of peatlands as dynamical systems. *Journal of Ecology*, 88(2), 230–242. <https://doi.org/10.1046/j.1365-2745.2000.00438.x>
- Hillel, D. (2004). *Introduction to environmental soil physics*. Amsterdam, NL: Elsevier Academic Press.
- Hoaglin, D. C., Iglewicz, B., & Tukey, J. W. (1986). Performance of some resistant rules for outlier labeling. *Journal of the American Statistical Association*, 81(396), 991–999. <https://doi.org/10.1080/01621459.1986.10478363>
- Hoeksema, R. J., Clapp, R. B., Thomas, A. L., Hunley, A. E., Farrow, N. D., & Dearstone, K. C. (1989). Cokriging model for estimation of water table elevation. *Water Resources Research*, 25(3), 429–438. <https://doi.org/10.1029/WR025i003p00429>
- Hughes, P. D. M., Mauquoy, D., Barber, K. E., & Langdon, P. G. (2000). Mire-development pathways and palaeoclimatic records from a full Holocene peat archive at Walton Moss, Cumbria, England. *The Holocene*, 10(4), 465–479. <https://doi.org/10.1191/095968300675142023>
- Ingram, H. A. P. (1982). Size and shape in raised mire ecosystems: A geophysical model. *Nature*, 297(5864), 300–303. <https://doi.org/10.1038/297300a0>
- Ivanov, K. E., Thomson, A., & Ingram, H. A. P. (1981). *Water movement in Mirelands*. London, UK: Academic Press.
- Jebara, T., Azarbajani, A., & Pentland, A. (1999). 3D structure from 2D motion. *Signal Processing Magazine, IEEE*, 16(3), 66–84. <https://doi.org/10.1109/79.768574>
- Journal, A. G., & Huijbregts, C. J. (1978). *Mining geostatistics*. London, UK: Academic press inc.
- Karofeld, E. (1998). The dynamics of the formation and development of hollows in raised bogs in Estonia. *The Holocene*, 8(6), 697–704. <https://doi.org/10.1191/095968398677584475>
- Kéfi, S., Guttal, V., Brock, W. A., Carpenter, S. R., Ellison, A. M., Livina, V. N., ... Dakos, V. (2014). Early warning signals of ecological transitions: Methods for spatial patterns. *PLoS ONE*, 9(3), e92097. <https://doi.org/10.1371/journal.pone.0092097>
- Kellner, E., & Halldin, S. (2002). Water budget and surface-layer water storage in a Sphagnum bog in central Sweden. *Hydrological Processes*, 16(1), 87–103. <https://doi.org/10.1002/hyp.286>
- Kemmers, R. H. (1986). *Perspectives in modelling of root zone of spontaneous vegetation at wet and damp sites in relation to regional water management* (Vol. 34). The Hague, Netherlands: Proc. Inf., CHO-TNO.
- Kennedy, G. W., & Price, J. S. (2004). Simulating soil water dynamics in a cutover bog. *Water Resources Research*, 40(12). <https://doi.org/10.1029/2004WR003099>
- Kennedy, G. W., & Price, J. S. (2005). A conceptual model of volume-change controls on the hydrology of cutover peats. *Journal of Hydrology*, 302(1–4), 13–27. <https://doi.org/10.1016/j.jhydrol.2004.06.024>
- Kettridge, N., & Binley, A. (2010). Evaluating the effect of using artificial pore water on the quality of laboratory hydraulic conductivity measurements of peat. *Hydrological Processes*, 24(18), 2629–2640. <https://doi.org/10.1002/hyp.7693>
- Kettridge, N., Turetsky, M. R., Sherwood, J. H., Thompson, D. K., Miller, C. A., Benscoter, B. W., ... Waddington, J. M. (2015). Moderate drop in water table increases peatland vulnerability to post-fire regime shift. *Scientific Reports*, 5. <https://doi.org/10.1038/srep08063>
- Kleinen, T., Brovkin, V., & Schuldt, R. J. (2012). A dynamic model of wetland extent and peat accumulation: Results for the Holocene. *Biogeosciences*, 9(1), 235–248. <https://doi.org/10.5194/bg-9-235-2012>
- Korpela, I., Koskinen, M., Vasander, H., Holopainen, M., & Minkinen, K. (2009). Airborne small-footprint discrete-return LiDAR data in the assessment of boreal mire surface patterns, vegetation, and habitats. *Forest Ecology and Management*, 258(7), 1549–1566. <https://doi.org/10.1016/j.foreco.2009.07.007>
- Korrensalo, A., Alekseychik, P., Hájek, T., Rinne, J., Vesala, T., Mehtätalo, L., ... Tuittila, E.-S. (2017). Species-specific temporal variation in photosynthesis as a moderator of peatland carbon sequestration. *Biogeosciences*, 14(2), 257–269. <https://doi.org/10.5194/bg-14-257-2017>
- Lafleur, P. M., Hember, R. A., Admiral, S. W., & Roulet, N. T. (2005). Annual and seasonal variability in evapotranspiration and water table at a shrub-covered bog in southern Ontario, Canada. *Hydrological Processes*, 19(18), 3533–3550. <https://doi.org/10.1002/hyp.5842>
- Lapen, D. R., Price, J. S., & Gilbert, R. (2005). Modelling two-dimensional steady-state groundwater flow and flow sensitivity to boundary

- conditions in blanket peat complexes. *Hydrological Processes*, 19(2), 371–386. <https://doi.org/10.1002/hyp.1507>
- Leach, J., Larsson, A., Wallin, M., Nilsson, M., & Laudon, H. (2016). Twelve year interannual and seasonal variability of stream carbon export from a boreal peatland catchment. *Journal of Geophysical Research: Biogeosciences*, 121(7), 1851–1866. <https://doi.org/10.1002/2016JG003357>
- Limpens, J., Berendse, F., Blodau, C., Canadell, J. G., Freeman, C., Holden, J., ... Schaepman-Strub, G. (2008). Peatlands and the carbon cycle: From local processes to global implications - a synthesis. *Biogeosciences*, 5(5), 1475–1491. <https://doi.org/10.5194/bg-5-1475-2008>
- Limpens, J., Holmgren, M., Jacobs, C. M. J., Van der Zee, S. E. A. T. M., Karofeld, E., & Berendse, F. (2014). How does tree density affect water loss of peatlands? A mesocosm experiment. *PLoS ONE*, 9(3), e91748. <https://doi.org/10.1371/journal.pone.0091748>
- van der Linden, M., Barke, J., Vickery, E., Charman, D. J., & van Geel, B. (2008). Late Holocene human impact and climate change recorded in a North Swedish peat deposit. *Palaeogeography, Palaeoclimatology, Palaeoecology*, 258(1–2), 1–27. <https://doi.org/10.1016/j.palaeo.2007.11.006>
- Lode, E., & Leivits, M. (2011). The LiDAR-based topo-hydrological modelling of the Nigula mire, SW Estonia. *Estonian Journal of Earth Sciences*, 60, 232–248. <https://doi.org/10.3176/earth.2011.4.04>
- Loisel, J., Yu, Z., Beilman, D. W., Camill, P., Alm, J., Amesbury, M. J., ... Zhou, W. (2014). A database and synthesis of northern peatland soil properties and Holocene carbon and nitrogen accumulation. *The Holocene*, 24, 1–15. <https://doi.org/10.1177/0959683614538073>
- Loreau, M., Naeem, S., Inchausti, P., Bengtsson, J., Grime, J. P., Hector, A., ... Wardle, D. A. (2001). Biodiversity and ecosystem functioning: Current knowledge and future challenges. *Science*, 294(5543), 804–808. <https://doi.org/10.2307/3085064>
- Lovitt, J., Rahman, M. M., & McDermid, J. G. (2017). Assessing the value of UAV photogrammetry for characterizing terrain in complex peatlands. *Remote Sensing*, 9(7). <https://doi.org/10.3390/rs9070715>
- Lucieer, A., Turner, D., King, D. H., & Robinson, S. A. (2014). Using an unmanned aerial vehicle (UAV) to capture micro-topography of Antarctic moss beds. *International Journal of Applied Earth Observation and Geoinformation*, 27, 53–62. <https://doi.org/10.1016/j.jag.2013.05.011>
- Luken, J. O. (1985). Zonation of Sphagnum mosses: Interactions among shoot growth, growth form, and water balance. *The Bryologist*, 88, 374–379. <https://doi.org/10.2307/3242680>
- Malhotra, A., Roulet, N. T., Wilson, P., Giroux-Bougard, X., & Harris, L. I. C. E. C. O. R. (2016). Ecohydrological feedbacks in peatlands: an empirical test of the relationship among vegetation, microtopography and water table. *Ecohydrology*, 9, 1346–1357. <https://doi.org/10.1002/eco.1731>
- Malmström, C. (1923). *Degerö Stormyr - En botanisk, hydrologisk och utvecklingshistorisk undersökning över ett nordsvenskt myrkomplex [IN SWEDISH]*. Stockholm, Sweden.
- Nijp, J. J., Limpens, J., Metselaar, K., Peichl, M., Nilsson, M. B., van der Zee, S. E. A. T. M., & Berendse, F. (2015). Rain events decrease boreal peatland net CO₂ uptake through reduced light availability. *Global Change Biology*, 21(6), 2309–2320. <https://doi.org/10.1111/gcb.12864>
- Nijp, J. J., Limpens, J., Metselaar, K., van der Zee, S., Berendse, F., & Robroek, B. J. M. (2014). Can frequent precipitation moderate the impact of drought on peatmoss carbon uptake in northern peatlands? *New Phytologist*, 203(1), 70–80. <https://doi.org/10.1111/nph.12792>
- Nijp, J. J., Metselaar, K., Limpens, J., Teutschbein, C., Peichl, M., Nilsson, M. B., ... van der Zee, S. E. A. T. M. (2017). Including hydrological self-regulating processes in peatland models: Effects on peatmoss drought projections. *Science of the Total Environment*, 580, 1389–1400. <https://doi.org/10.1016/j.scitotenv.2016.12.104>
- Nijp, J. J., Temme, A. J. A. M., Voorn, G. A. K. V., Kooistra, L., Hengeveld, G. M., Soons, M. B., ... Wallinga, J. (2019). Spatial early warning signals for impending regime shifts: A practical framework for application in real-world landscapes. *Global Change Biology*. <https://doi.org/10.1111/gcb.14591>
- Nilsson, M., & Öquist, M. (2009). Partitioning litter mass loss into carbon dioxide and methane in peatland ecosystems. In *Carbon cycling in northern peatlands* (pp. 131–144). Washington, DC: American Geophysical Union.
- Nilsson, M., Sagerfors, J., Buffam, I., Laudon, H., Eriksson, T., Grelle, A., ... Lindroth, A. (2008). Contemporary carbon accumulation in a boreal oligotrophic minerogenic mire - a significant sink after accounting for all C-fluxes. *Global Change Biology*, 14(10), 2317–2332. <https://doi.org/10.1111/j.1365-2486.2008.01654.x>
- Nungesser, M. K. (2003). Modelling microtopography in boreal peatlands: hummocks and hollows. *Ecological Modelling*, 165(2–3), 175–207. [https://doi.org/10.1016/S0304-3800\(03\)00067-X](https://doi.org/10.1016/S0304-3800(03)00067-X)
- Oosterwoud, M., Ploeg, M., Schaaf, S., & van der Zee, S. (2017). Variation in hydrologic connectivity as a result of microtopography explained by discharge to catchment size relationship. *Hydrological Processes*, 31(15), 2683–2699. <https://doi.org/10.1002/hyp.11164>
- Päivänen, J. (1982). Physical properties of peat samples in relation to shrinkage upon drying. *Silva Fennica*, 16(3), 247–265.
- Pebesma, E. J. (2004). Multivariable geostatistics in S: The gstat package. *Computers & Geosciences*, 30, 683–691. <https://doi.org/10.1016/j.cageo.2004.03.012>
- Peel, M. C., Finlayson, B. L., & McMahon, T. A. (2007). Updated world map of the Köppen-Geiger climate classification. *Hydrology and Earth System Sciences*, 11(5), 1633–1644. <https://doi.org/10.5194/hess-11-1633-2007>
- Peichl, M., Öquist, M., Löfvenius, M. O., Ilstedt, U., Sagerfors, J., Grelle, A., ... Nilsson, M. B. (2014). A 12-year record reveals pre-growing season temperature and water table level threshold effects on the net carbon dioxide exchange in a boreal fen. *Environmental Research Letters*, 9(5), 055006. <https://doi.org/10.1088/1748-9326/1089/1085/055006>
- Peichl, M., Sagerfors, J., Lindroth, A., Buffam, I., Grelle, A., Klemetsson, L., ... Nilsson, M. B. (2013). Energy exchange and water budget partitioning in a boreal minerogenic mire. *Journal of Geophysical Research - Biogeosciences*, 118(1), 1–13. <https://doi.org/10.1029/2012JG002073>
- Peterson, G., Allen, C. R., & Holling, C. S. (1998). Ecological resilience, Biodiversity, and Scale. *Ecosystems*, 1(1), 6–18. <https://doi.org/10.1007/s100219900002>
- Petrone, R., Devito, K., Silins, U., Mendoza, C., Brown, S., Kaufman, S., & Price, J. (2008). Transient peat properties in two pond-peatland complexes in the sub-humid Western Boreal Plain, Canada. *Mires & Peat*, 3, 1–13.
- Price, J. S. (2003). Role and character of seasonal peat soil deformation on the hydrology of undisturbed and cutover peatlands. *Water Resources Research*, 39, 1241–1251.
- Price, J. S., Cagampan, J., & Kellner, E. (2005). Assessment of peat compressibility: is there an easy way? *Hydrological Processes*, 19(17), 3469–3475. <https://doi.org/10.1002/hyp.6068>
- Qiu, C., Zhu, D., Ciais, P., Guenet, B., Krinner, G., Peng, S., ... Ziemblinska, K. (2018). ORCHIDEE-PEAT (revision 4596), a model for northern peatland CO₂, water and energy fluxes on daily to annual scales. *Geoscientific Model Development*, 11, 497–519. <https://doi.org/10.5194/gmd-2017-155>
- Quinton, W. L., & Roulet, N. T. (1998). Spring and summer runoff hydrology of a subarctic patterned wetland. *Arctic and Alpine Research*, 30(3), 285–294. <https://doi.org/10.1080/00040851.1998.12002902>

- R Core Team (2018). *R: A language and environment for statistical computing*. Vienna, Austria: R Foundation for Statistical Computing. Retrieved from <http://www.R-project.org/>
- Rakovec, O., Hazenberg, P., Torfs, P. J. J. F., Weerts, A. H., & Uijlenhoet, R. (2012). Generating spatial precipitation ensembles: Impact of temporal correlation structure. *Hydrology and Earth System Sciences*, 16(9), 3419–3434. <https://doi.org/10.5194/hess-16-3419-2012>
- Rietkerk, M., Dekker, S. C., de Ruiter, P. C., & van de Koppel, J. (2004). Self-organized patchiness and catastrophic shifts in ecosystems. *Science*, 305(5692), 1926–1929. <https://doi.org/10.1126/science.1101867>
- Rossi, R. E., Mulla, D. J., Journel, A. G., & Franz, E. H. (1992). Geostatistical tools for modeling and interpreting ecological spatial dependence. *Ecological Monographs*, 62(2), 277–314. <https://doi.org/10.2307/2937096>
- Roulet, N. T. (1991). Surface level and water table fluctuations in a subarctic fen. *Arctic and Alpine Research*, 23(3), 303–310. <https://doi.org/10.2307/1551608>
- Rydin, H. (1986). Competition and niche separation in Sphagnum. *Canadian Journal of Botany*, 64(8), 1817–1824. <https://doi.org/10.1139/b86-240>
- Rydin, H., & Jeglum, J. R. (2013). *The biology of peatlands* (2nd ed.). Oxford, United Kingdom: Oxford University Press.
- Scheffer, M., Carpenter, S., Foley, J. A., Folke, C., & Walker, B. (2001). Catastrophic shifts in ecosystems. *Nature*, 413(6856), 591–596. <https://doi.org/10.1038/35098000>
- Scherrer, D., & Körner, C. (2011). Topographically controlled thermal-habitat differentiation buffers alpine plant diversity against climate warming. *Journal of Biogeography*, 38(2), 406–416. <https://doi.org/10.1111/j.1365-2699.2010.02407.x>
- Schilling, W. (1991). Rainfall data for urban hydrology: What do we need? *Atmospheric Research*, 27(1–3), 5–21. [https://doi.org/10.1016/0169-8095\(91\)90003-f](https://doi.org/10.1016/0169-8095(91)90003-f)
- Schlotzhauer, S. M., & Price, J. S. (1999). Soil water flow dynamics in a managed cutover peat field, Quebec: Field and laboratory investigations. *Water Resources Research*, 35(12), 3675–3683. <https://doi.org/10.1029/1999WR900126>
- Sjörs, H. (1948). Myrvegetation i Bergslagen. [Mire vegetation in Bergslagen, Sweden.]. *Acta Phytogeographica Suecica*, 21, 1–299.
- Sonnentag, O., Chen, J. M., Roulet, N. T., Ju, W., & Govind, A. (2008). Spatially explicit simulation of peatland hydrology and carbon dioxide exchange: Influence of mesoscale topography. *Journal of Geophysical Research: Biogeosciences*, 113(G2), G02005. <https://doi.org/10.1029/2007jg000605>
- Suzuki, R., & Shimodaira, H. (2006). Pvcust: An R package for assessing the uncertainty in hierarchical clustering. *Bioinformatics*, 22(12), 1540–1542. <https://doi.org/10.1093/bioinformatics/btl117>
- Terzaghi, K. (1943). *Theoretical soil mechanics*. New York, US: John Wiley & Sons. <https://doi.org/10.1002/9780470172766>
- Turunen, J., Tomppo, E., Tolonen, K., & Reinikainen, A. (2002). Estimating carbon accumulation rates of undrained mires in Finland-application to boreal and subarctic regions. *The Holocene*, 12(1), 69–80. <https://doi.org/10.1191/0959683602hl522rp>
- Uhden, E. H. O. (1967). Niederschlags- und Abflußbeobachtungen auf unberührten, vorentwässerten und kultivierten Teilen eines nordwestdeutschen Hochmoores der Esterweger Dose am Küstkanal bei Papenburg [GERMAN] Rainfall- and discharge observations on pristine, drained and cultivated parts of a Northwestern German bog in the Esterweger Dose at the Küsten Canal near Papenburg. Hamburg, Germany: Verlag Wasser und Boden.
- Waddington, J. M., Kellner, E., Strack, M., & Price, J. S. (2010). Differential peat deformation, compressibility, and water storage between peatland microforms: Implications for ecosystem function and development. *Water Resources Research*, 46(7), W07538. <https://doi.org/10.1029/2009WR008802>
- Waddington, J. M., Morris, P. J., Kettridge, N., Granath, G., Thompson, D. K., & Moore, P. A. (2015). Hydrological feedbacks in northern peatlands. *Ecohydrology*, 8(1), 113–127. <https://doi.org/10.1002/eco.1493>
- Webster, R., & Oliver, M. A. (2007). *Geostatistics for environmental scientists*. Chichester, England: John Wiley & Sons. <https://doi.org/10.1002/9780470517277>
- Whittington, P., Strack, M., van Haarlem, R., Kaufman, S., Stoesser, P., Maltez, J., ... Stone, M. (2007). The influence of peat volume change and vegetation on the hydrology of a kettle-hole wetland in Southern Ontario, Canada. *Mires and Peat*, 2, 1–14.
- Whittington, P. N., & Price, J. S. (2006). The effects of water table draw-down (as a surrogate for climate change) on the hydrology of a fen peatland, Canada. *Hydrological Processes*, 20(17), 3589–3600. <https://doi.org/10.1002/hyp.6376>
- Yu, Z. (2011). Holocene carbon flux histories of the world's peatlands: Global carbon-cycle implications. *Holocene*, 21(5, SI), 761–774. <https://doi.org/10.1177/0959683610386982>
- Zlotnik, V. A., Goss, D., & Duffield, G. M. (2010). General steady-state shape factor for a partially penetrating well. *Ground Water*, 48(1), 111–116. <https://doi.org/10.1111/j.1745-6584.2009.00621.x>

SUPPORTING INFORMATION

Additional supporting information may be found online in the Supporting Information section at the end of the article.

How to cite this article: Nijp JJ, Metselaar K, Limpens J, et al. High-resolution peat volume change in a northern peatland: Spatial variability, main drivers, and impact on ecohydrology. *Ecohydrology*. 2019;12:e2114. <https://doi.org/10.1002/eco.2114>